Raman lasing near 630 nm from stationary glycerol–water microdroplets on a superhydrophobic surface

A. Sennaroglu,[1,3] A. Kiraz,[1,4] M. A. Dündar,[1] A. Kurt,[1] and A. L. Demirel[2]

[1]*Department of Physics, Koç University, Rumelifeneri Yolu, 34450 Sariyer, Istanbul, Turkey*
[2]*Department of Chemistry, Koç University, Rumelifeneri Yolu, 34450 Sariyer, Istanbul, Turkey*
[3]*Corresponding author: asennar@ku.edu.tr*
[4]*akiraz@ku.edu.tr*

Received March 23, 2007; revised June 7, 2007; accepted June 8, 2007;
posted June 18, 2007 (Doc. ID 81429); published July 24, 2007

We demonstrate, for the first time to our knowledge, Raman lasing from stationary microdroplets on a superhydrophobic surface. In the experiments, glycerol–water microdroplets with radii in the 11–15 μm range were pumped at 532 nm with a pulsed, frequency-doubled Nd:YAG laser. Two distinct operation regimes of the microdroplets were observed: cavity-enhanced Raman scattering and Raman lasing. In the latter case, the Raman lasing signal was higher than the background by more than 30 dB. Investigation of the Raman spectra of various glycerol–water mixtures indicates that lasing occurs within the glycerol Raman band. Raman lasing was not sustained; rather, oscillation would occur in temporally separated bursts. Increasing the rate of convective cooling by nitrogen purging improved the lasing performance and reduced the average interburst separation from 2.3 to 0.4 s. © 2007 Optical Society of America

OCIS codes: 140.3550, 350.3950, 230.3990, 230.5750, 190.5650.

Recently, there has been a great deal of interest in the development of compact light sources based on optical microcavities [1–8]. By using these structures, light at the resonant frequencies can be confined to very small volumes. In addition, because very high cavity quality (Q) factors can be achieved, low-threshold optical oscillation is possible. Potential applications of microcavities are diverse, ranging from fundamental studies of cavity quantum electrodynamics to optical communications [5] and determination of size and chemical composition of aerosols [6], to name a few. In optical communications, microcavity lasers emitting near 1550 nm are very important in silica-based fiber-optic systems. Another important wavelength range is around 650 nm, corresponding to one of the low-loss transmission windows of the short-haul communications systems employing plastic fibers [9].

Lasing from microcavities can be obtained by introducing resonant gain inside the cavity with, for example, fluorescent dyes [1], quantum dots [10], rare earth ions [11], or quantum wells [12], or by employing a nonlinear signal generation scheme such as Raman scattering [2]. In previous studies, low-threshold Raman lasing has been successfully demonstrated in microcavities made of solid-state transparent media such as silica [4,8] and CaF_2 [13]. Extensive studies have also been performed to investigate resonant Raman scattering in liquid microdroplet streams [2], electrodynamically levitated microparticles [14], or optically trapped liquid microdroplets [7]. However, to date, only cavity-enhanced Raman scattering (CERS) has been reported with microdroplets. In addition, resonant Raman emission characteristics of stationary microdroplets located on a surface have not been reported. This is in part due to the challenge of properly optimizing the surface characteristics to minimize the geometric deformation of the otherwise spherical droplet and at the same time to maintain a sufficiently high Q factor for the resonant modes.

In this work, we demonstrate, for the first time to our knowledge, Raman lasing from stationary microdroplets situated on a superhydrophobic surface. In the experiments, we identified two distinct regimes of operation by using glycerol–water microdroplets on a superhydrophobic surface: CERS and Raman lasing. In the latter case, the estimated contrast ratio between the Raman signal peak and the background was larger than 30 dB. Raman lasing was not sustained; rather oscillation occurred in temporally separated bursts. Observations indicated that increasing the rate of convective cooling via nitrogen purging reduced the interbust separation from 2.3 to 0.4 s.

Superhydrophobic surfaces were prepared by spin-coating hydrophobically coated silica nanoparticles as described previously [15]. Glycerol–water microdroplets were generated by spraying a 12.5% or 25% glycerol–water solution onto the superhydrophobic surface using either an atomizer or an ultrasonic nebulizer under ambient humidity. A Q-switched, frequency-doubled Nd:YAG laser ($\lambda = 532$ nm, pulse width = 100 ns, pulse repetition rate = 1 kHz, average power = 60 mW) was used for excitation. The excitation beam was focused to an estimated 28-μm-diameter spot by using a microscope objective (NA = 0.88, 60×) in the inverted geometry. In recording the Raman spectra, scattered intensity was collected with the same microscope objective and sent through the dichroic mirror, a 1.5× magnification element, and a long-pass filter. The signal was then dispersed by a monochromator (300 grooves/mm grating, spectral resolution = 0.24 nm) and detected by a CCD camera.

0146-9592/07/152197-3/$15.00

With smaller microdoplets, generated using the ultrasonic nebulizer, we were able to observe CERS. Figure 1 shows the CERS spectrum of a 10.9-μm-diameter microdroplet, recorded using a total exposure time of 45 s. In this spectrum, the whispering gallery modes (WGMs) are clearly visible together with the Raman emission bands of the glycerol–water solution. For the WGMs shown in Fig. 1, free spectral ranges (FSRs) of 10.6 and 10.8 nm are measured, indicated by A and B, respectively. For a 10.9-μm-diameter ideal glycerol microsphere, an FSR of 8.9 nm is expected. The deviation of the observed FSRs from 8.9 nm is due to the nonspherical geometry of the microdroplet standing on a superhydrophobic surface [15]. Despite the high excitation power, none of the WGMs dominated the spectrum and hence no clear evidence for Raman lasing was observed. The absence of lasing is mainly attributed to low Q factors of the WGMs of smaller microdroplets. The full width at half-maximum of the WGMs revealed Q factors of up to ~2000 in this case.

Raman lasing was routinely observed in larger microdroplets generated with the atomizer. As an example, Fig. 2 shows the spectra obtained from a 12.4-μm-diameter microdroplet, showing Raman lasing. During a series of consecutive acquisitions, intense WGM emission is momentarily observed in the high-gain region of the Raman bands at 632.3 nm, as shown in Fig. 2(a). This is a clear indication of Raman lasing. Raman lasing is not sustained, and the intensity of the lasing WGM drops by more than 30 dB in the consecutive acquisition [Fig. 2(b)]. The inset in Fig. 2(a) shows the "on/off" behavior observed during 20 acquisitions for this microdroplet. At acquisitions 7, 9, and 13, high-intensity Raman lasing is observed, while the collected intensity is much smaller during the remaining acquisitions. Despite the "on/off" behavior, the spectral location of the lasing WGM remains stable, indicating a constant droplet size within the spectral resolution of the measurement setup.

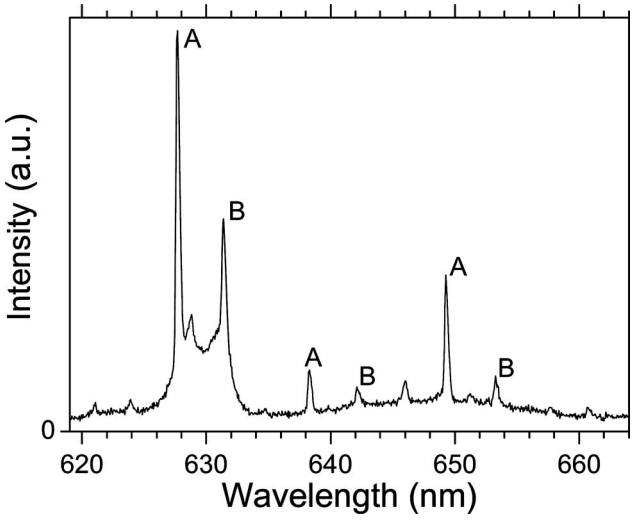

Fig. 1. Cavity-enhanced Raman scattering spectrum of a 10.9-μm-diameter glycerol–water microdroplet. Exposure time is 45 s.

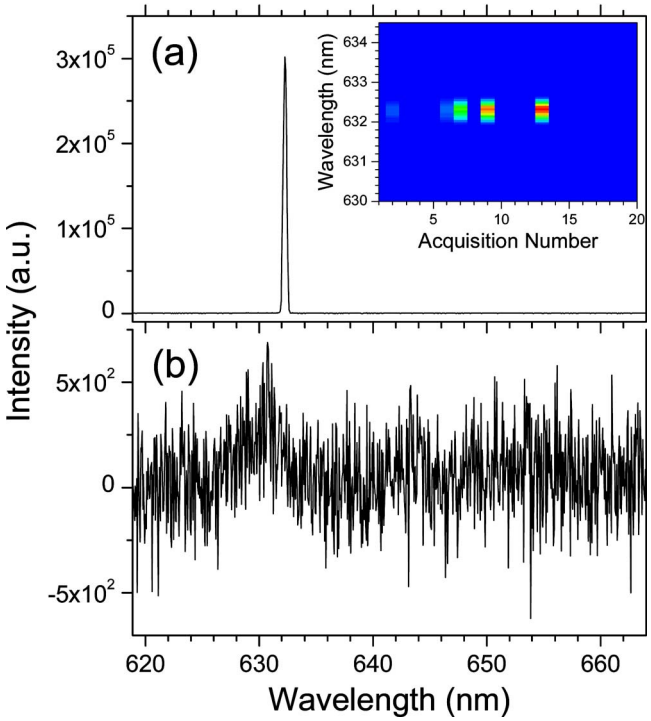

Fig. 2. (Color online) (a) Measured spectrum obtained from a 12.4-μm-diameter microdroplet, showing Raman lasing. (b) Corresponding spectrum during the nonlasing period. The inset shows the consecutive spectra (exposure time=1 s) showing the "on–off" behavior.

To investigate the origin of Raman lasing, we recorded the Raman spectra of glycerol–water mixtures of various compositions. Figure 3 shows the acquired spectra for solutions containing (curve A) 100 and (curve B) 13 vol.% water. As can be seen, the band centered around 630 nm originates from glycerol and dominates in the mixture containing 13 vol.% water. Even in a mixture containing 50 vol.% water (not shown in Fig. 3), the peak of the glycerol band near 630 nm was larger than that of the 650 nm band by more than 60%. After reaching the equilibrium sizes, the investigated microdroplets have a Raman spec-

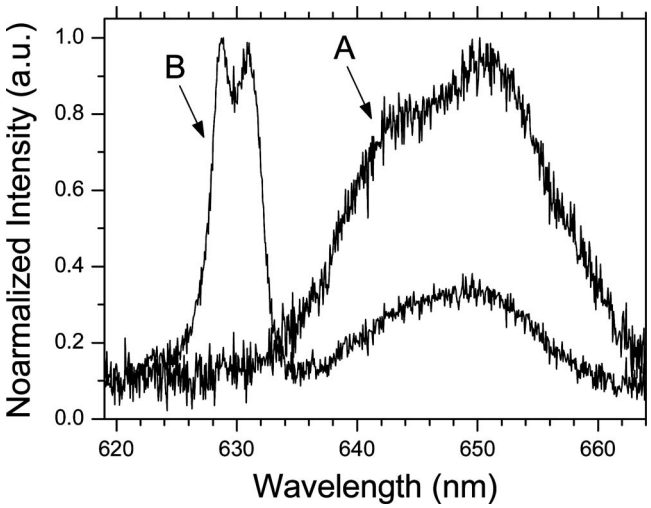

Fig. 3. Normalized Raman spectra of glycerol–water mixtures containing (curve A) 100, and (curve B) 13 vol.% water. Exposure time is 30 s.

trum similar to that in curve B of Fig. 3. Hence, this indicates that Raman lasing occurs due to the presence of glycerol, which has a larger Raman gain in the 620–660 nm spectral window (see Fig. 3).

Without an exception, "on/off" behavior was observed in all microdroplets showing Raman lasing. This phenomenon is possibly due to thermally induced density fluctuations during lasing. As a result, the circulating mode acquires a spatially distorted phase and can no longer satisfy the resonance condition. During the "off" period, excess generated heat is dissipated and Raman lasing resumes once the microdroplet cools down. Detailed experiments performed with the lasing microdroplets suggest that heat dissipation is limited by the rate of convective cooling. To test this hypothesis further, we investigated the lasing characteristics of a 21.5-μm-diameter microdroplet with and without nitrogen purging. Figure 4 shows the Raman lasing intensity as a function of time. This time trace was generated by analyzing the video of the Raman signal collected from the microdroplet (recorded at a rate of 25 frames/s). At each frame, intensity was calculated by integrating the brightness over a box including the microdroplet. The box used in calculating the time trace is shown in Fig. 4 at three different frames. The ring pattern of the lasing mode is visible in frames 3348 and 12,083, while very low intensity is collected in frame 3349, corresponding to an "off" period. As can be seen in Fig. 4, during the purging intervals, average interburst separation was observed to decrease from 58.6 frames (2.3 s) to 10.2 frames (0.4 s), believed to be due to increased convective cooling efficiency.

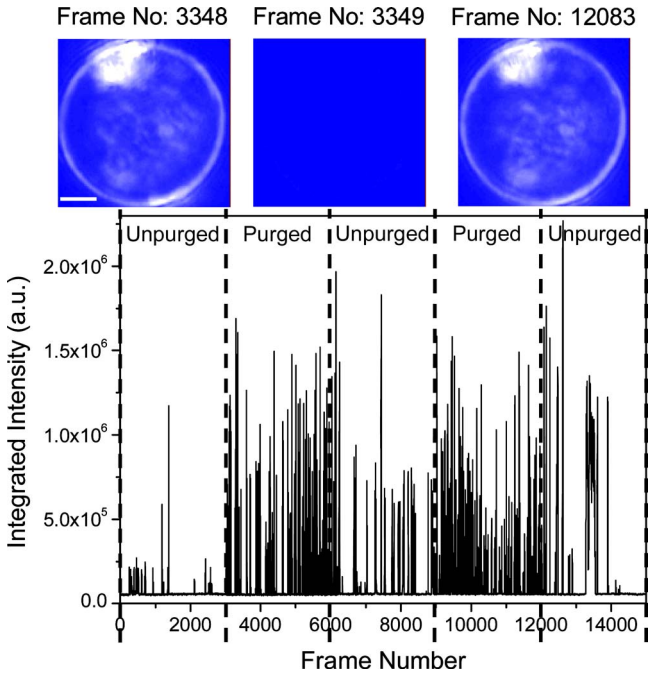

Fig. 4. (Color online) Recorded time trace of the Raman lasing intensity observed from a 21.5-μm-diameter microdroplet. The recording rate is 25 frames/s. Images used in calculating the time trace at frames 3348, 3349, and 12,083 are shown at the top. The scale bar shows 5 μm.

In conclusion, we have observed CERS and Raman lasing from stationary, glycerol–water microdroplets situated on a superhydrophobic surface. Measurements gave a clear indication of Raman lasing within the Raman band of glycerol, not previously observed in other studies with microdroplets. Raman lasing was, however, not sustained and occurred in temporally separated bursts. We note that the novel configuration based on the superhydrophobic surface obviates the need for additional trapping schemes such as electrodynamic levitation and optical trapping [7,14]. Finally, the system described here could become a compact, cost-effective light source for short-haul communications systems.

This work was supported by the Scientific and Technological Research Council of Turkey (Grant No. TÜBİTAK-105T500). The authors thank H. Kalaycioglu and S. Doğanay for their assistance. The authors are also grateful to the Alexander von Humboldt Foundation for equipment donation. A. Kiraz further acknowledges the financial support of the Turkish Academy of Sciences in the framework of the Young Scientist Award program (Grant No. A.K/TÜBA-GEBİP/2006-19).

References

1. H.-M. Tzeng, K. F. Wall, M. B. Long, and R. K. Chang, Opt. Lett. **9**, 499 (1984).
2. J. B. Snow, S.-X. Qian, and R. K. Chang, Opt. Lett. **10**, 37 (1985).
3. A. S. Kwok, A. Serpengüzel, W.-F. Hsieh, R. K. Chang, and J. B. Gillespie, Opt. Lett. **17**, 1435 (1992).
4. S. M. Spillane, T. J. Kippenberg, and K. J. Vahala, Nature **415**, 621 (2002).
5. K. J. Vahala, Nature **424**, 839 (2003).
6. R. J. Hopkins, R. Symes, R. M. Sayer, and J. P. Reid, Chem. Phys. Lett. **380**, 665 (2003).
7. R. J. Hopkins, L. Mitchem, A. D. Ward, and J. P. Reid, Phys. Chem. Chem. Phys. **6**, 4924 (2004).
8. A. Mazzei, H. Krauter, O. Benson, and S. Gotzinger, Appl. Phys. Lett. **89**, 101105 (2006).
9. M. M. Dimitrescu, M. J. Saarinen, M. D. Guina, and M. V. Pessa, IEEE J. Quantum Electron. **8**, 219 (2002).
10. P. Michler, A. Kiraz, L. Zhang, C. Becher, E. Hu, and A. Imamoglu, Appl. Phys. Lett. **77**, 184 (2000).
11. V. Sandoghdar, F. Treussart, J. Hare, V. Lefevre-Seguin, J.-M. Raimond, and S. Haroche, Phys. Rev. A **54**, R1777 (1996).
12. A. C. Tamboli, E. D. Haberer, R. Sharma, K. H. Lee, S. Nakamura, and E. L. Hu, Nat. Photonics **1**, 61 (2006).
13. I. S. Grudunin and L. Maleki, Opt. Lett. **32**, 166 (2007).
14. S. Arnold and L. M. Folan, Rev. Sci. Instrum. **57**, 2250 (1986).
15. A. Kiraz, A. Kurt, M. A. Dundar, and A. L. Demirel, Appl. Phys. Lett. **89**, 081118 (2006).